Robotic Assisted MRI-Guided Interventional interstitial MR Guided Focused Ultrasound Ablation in a Swine Model

Jacquelyn MacDonell MS; Niravkumar Patel PhD; Gregory S Fischer PhD; E. Clif Burdette PhD; Jiang Qian MD; Vaibhav Chumbalkar MBBS; Goutam Ghoshal PhD; Tamas Heffter MSc; Emery Williams; Matthew J Gounis PhD; Juliette Thibodeau; Gene Bogdanov PhD; Robert M. King BS; Olivia W Brooks BS; Erin Langan BS; Roy S Hwang; Julie G. Pilitsis MD PhD

CNS
2018 ANNUAL MEETING
HOUSTON, TEXAS
OCTOBER 6-10, 2018

BACKGROUND

Current therapies for brain metastasis include surgical resection, whole brain radiation therapy, stereotactic radiosurgery and chemotherapy. Ablative therapies such as laser interstitial thermal therapy (LITT) and transcranial magnetic resonance guided focused ultrasound (tcMRgFUS) have been proposed as treatment alternatives for brain metastasis. Laser penetration in LITT is limited by carbonization of adjacent tissue leading to incomplete ablation rates with larger tumor volumes. Similarly, tcMRgFUS is limited to small tumor volumes as large volumes may result in overheating of the skull.

We propose interstitial MR guided focused ultrasound (iMRgFUS) as an alternative ablative technique for the treatment of brain metastasis and have developed an MRI-Guided robotic assistant (MRgRA) to deliver this therapy.

METHODS

In an initial three animals, we optimized the workflow of the robot in the MR suite and made modifications to the robotic arm to allow range of motion. Then, six farm pigs (4 acute, 2 survival) underwent 7 iMRgFUS ablations using MRgRA. We altered dosing to explore differences between thermal dosing in brain as compared to other tissues. Imaging were compared to gross examination. Our work culminated in adjustments to the MRgRA, iMRgFUS probes and dosing, culminating in 2 survival surgeries; swine had ablations with no neurological sequelae at 2 weeks postprocedure.

METHODS (CONT.)

Immediately following iMRgFUS therapy, DWI and T1 weighted MR were accurate reflections of the ablation volume. T2 and FLAIR images were accurate reflections of ablation volume 1week post procedure. We successfully performed MRgRA iFUS ablation in swine and found intraoperative and post-operative imaging to correlate with histological examination. These data are useful to validate our system and to guide imaging follow-up for thermal ablation lesions in brain tissue from our therapy, tcMRgFUS, and LITT.

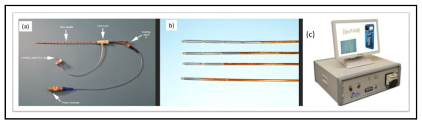

FIGURE 1- (ABOVE) iMRgFUS Ultrasound Probe and TheraVision™ Ultrasound Thermal Therapy System. (a) Photo of an applicator inserted into a catheter used for the experiment, (b) fabricated ultrasound applicators with one, two, three and four transducers, (c) TheraVision™ ultrasound thermal therapy system with 1-4 RF output channels used to power each transducer element.

METHODS (CONT.)

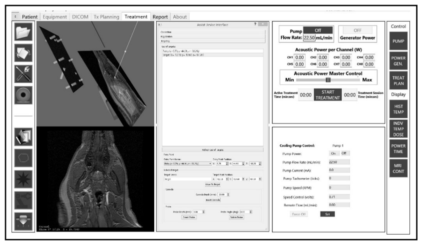

FIGURE 2- Registering the Robotic Assistant to MRI. Registration of the robot using multiple coronal images of the fiducial frame (top left image). By attaching the fiducial frame to the robot and then acquiring a stack of coronal images, the registration transformation from the image coordinate system and the robot coordinate system is determined using software algorithms developed during this program.

FIGURE 3- Creating a Sterile Field Within the MRI Bore. (a) Robotic manipulator and base platform without draping. (b) Sterile environment for survival surgeries created by draping both the animal and robot manipulator in a sterile plastic sheet. Wires and tubing leaving the robot manipulator were wrapped in a sterile surgical cloth that was secured by zip ties.

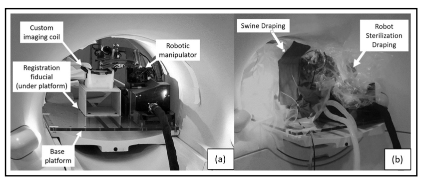

METHODS (CONT.)

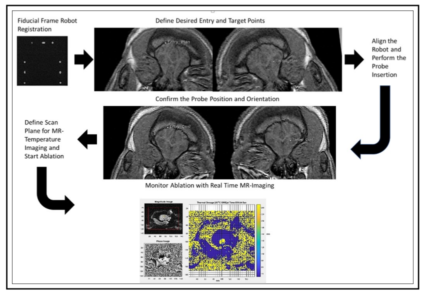

FIGURE 4- Imaging Workflow. MR images used throughout the procedure starting with fiducial frame robot registration (top left) and ending with Magnetic Resonance Thermal Imaging (MRTI) (bottom)

FIGURE 5- Custom Wire Surface Coil For Pig Brain Imaging. (a) computer-aided design (CAD) model, (b) prototype with insulation and wires bent into the desired shape.

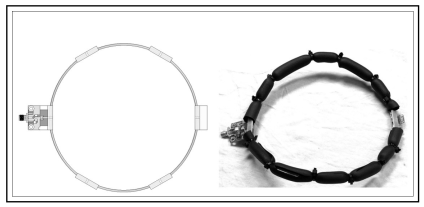

RESULTS

Surgery	Experimental Group	Acoustic Output Power (Watts)	Duration Right Frontal or Temporal Lobe (Seconds)	Duration Left Frontal or Temporal Lobe (Seconds)	Predicted Ablation Volume (cm^3)
1	Acute	4	180	N/A	4.26
2	Acute	4	180	120	L: 4.26 R: 2.21
3	Acute	6	180	N/A	5.20
4*	Acute	3	N/A	150	1.63
5*	Survival	4ᵗ	120	N/A	-
6*	Survival	3	100	N/A	0.44

*: Used 360 ablator probe with 7mm element instead of 10mm element
t: TheraVision software system became unresponsive during HIFU treatment and was manually shut off. Watts delivered during that time is unknown

FIGURE 1- (ABOVE) Acoustic Output and Ablation Time. Each animal was placed in either an acute or survival group. Acute animals were sacrificed post ablation. Survival animals were monitored for a two week period post ablation. Acoustic output power was measured in watts and ablation duration in seconds.

RESULTS (CONT.)

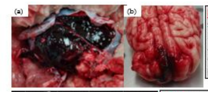

Fig 6. Post-examination revealing subarachnoid blood. (a) Sub-dural Hematoma observed during extraction of acute animals. (b) Post extraction examination revealing damage to frontal pole.

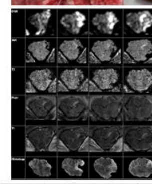

Fig 7. MR Imaging Compared to Gross Histology at tp0. Comparison of MRI imaging sequence to histological section for an acute surgery where Triphenyl Tetrazolium Chloride (TTC) staining methods were utilized. Each row represents a different MR-Imaging sequence taken at tp0. Each column represents an MRI slice taken at the same location as the histological section.

Table 2. (BELOW) Ablation Volumes on MRI Compared to Pathology at tp0. Ablation volumes immediately following ablation (tp0) compared to predicted ablation volumes and pathologic findings.

Surgery tp0	DWI	SWI	T1*	T2	FLAIR	Histology	Predicted
1	8.23 cm^3	1.49 cm^3	8.16 cm^3	x	x	8.61 cm^3	4.46 cm^3
2 Right	1.41 cm^3	n/a	X	n/a	n/a	0.87 cm^3	4.16 cm^3
2 Left	2.35 cm^3	n/a	2.79* cm^3	n/a	n/a	1.52 cm^3	2.21 cm^3
3	0.31 cm^3	n/a	X	n/a	n/a	0.12 cm^3	5.20 cm^3
4*	0.32 cm^3	n/a	X	n/a	n/a	0.27 cm^3	1.63 cm^3
5*	0.17 cm^3	n/a	X	n/a	n/a	0.10 cm^3	-
6*	0.43 cm^3	0.23 cm^3	0.25 cm^3	x	x	0.24 cm^3	0.44 cm^3

n/a: MR-sequence not available
x: Sequence did not demonstrate ablation
* Indicates gadolinium

Surgery	DWI	SWI	T1*	T2	Flair	Histology	Predicted
5 tp0	0.17 cm^3	n/a	X*	n/a	n/a		-
5 tp1	0.49 cm^3	1.28 cm^3	0.61* cm^3	0.24 cm^3	0.35 cm^3		-
5 tp2	0.23 cm^3	0.91 cm^3	0.55 cm^3	0.29 cm^3	0.36 cm^3	0.10 cm^3	-
6 tp0	0.43 cm^3	0.23 cm^3	0.25* cm^3	X	X		0.44 cm^3
6 tp1	x	0.52 cm^3	0.07* cm^3	0.06 cm^3	0.2 cm^3		0.44 cm^3
6 tp2	x	0.30 cm^3	X*	x	0.09 cm^3	0.24 cm^3	0.44 cm^3

n/a: MR-sequence not available
x: Sequence did not demonstrate ablation
* Indicates gadolinium

Table 3. (ABOVE) Table 3.4 Ablation Volumes on MRI Compared to Histology in survival animals. Ablation volumes immediately following ablation (tp0), 1 week post ablation (tp1) and two weeks post ablation (tp2) were measured four times by two different observers. An average of the four measurements was used as the true volume.

CONCLUSION

We successfully performed 7 iMRgFUS ablations using MRgRA on 5 acute and 2 survival animals. Throughout the course of the experiments probes and dosing of iMRgFUS were optimized. DWI and T1 were available on all animals at tp0 and tp1 and both were accurate reflections of the ablation volume . DWI only demonstrated ablation on one survival surgery but was an accurate reflection of ablation volume at both tp1 and tp2. SWI was a poor reflection of ablation volume at tp0 but became more accurate at tp1 and tp2. Flair was the most accurate reflection of ablation volume at tp2 and was additionally able to identify edema.

REFERENCES

(SEE ATTACHED)